Temporal Pattern Recognition in Gait Activities Recorded With a Footprint Imaging Sensor System

Omar Costilla-Reyes, Patricia Scully, and Krikor B. Ozanyan, *Senior Member, IEEE*

***Abstract*— In this paper, we assess the capability of a unique unobtrusive footprint imaging sensor system, based on plastic optical fiber technology, to allow efficient gait analysis from time domain sensor data by pattern recognition techniques. Trial gait classification experiments are executed as ten manners of walking, affecting the amplitude and frequency characteristics of the temporal signals. The data analysis involves the design of five temporal features, subsequently analyzed in 14 different machine learning models, representing linear, non-linear, ensemble, and deep learning models. The model performance is presented as cross-validated accuracy scores for the best model-feature combinations, along with the optimal hyper-parameters for each of them. The best classification performance was observed for a random forest model with the adjacent mean feature, yielding a mean validation score of 90.84% ± 2.46%. We conclude that the floor sensor system is capable of detecting changes in gait by means of pattern recognition techniques applied in the time domain. This suggests that the footprint imaging sensor system is suitable for gait analysis applications ranging from healthcare to security.**

***Index Terms*— Floor sensor, sensor fusion, gait analysis, pattern recognition, machine learning.**

I. Introduction

GAIT analysis has a wide range of applications: from biometrics [1] in security applications to monitoring of human movement in sports and healthcare [2]. Typically, both temporal and spatial parameters of gait, such as cadence, stride length and walking base are analyzed from data acquired by a suitable sensor system or fused from several systems. This paper presents the first demonstration of time-domain gait analysis using a new type of footprint imaging sensor ("Intelligent Carpet") based on plastic optical fibers (POFs) sensitive to deformation when pressure is applied by walking. The system is an innovative cost-efficient combination of hardware and software resulting in a novel non-planar tomographic technique [3] allowing real-time reconstruction of footsteps on the surface of an ordinary carpet [4]. Deployed over typical living space areas, it offers substantial advantages in cost and measurement efficiency compared to other floor sensor systems, such as the commercial TekScan [5] and GAITRite [6]. The footprint imaging sensor is intrinsically safe and robust against light or sound interference that affects alternatives such as sound or vision sensors [7]. The adoption of these alternatives in a home environment is further hampered by privacy concerns [8].

Due to its unobtrusiveness, the footprint imaging sensor can collect natural gait and movement outside the laboratory or clinical setting [9]. This allows footprint time sequences to be recorded, stored and analyzed over practically unlimited periods of time, as opposed to scheduled sessions, without affecting the users' perception of their everyday environment. Thus, the large volume of data available from the footprint imaging sensor allows gait analysis, by using machine learning models.

The objective of this work is to distinguish and classify, different manners of walking by machine learning models. To the best of our knowledge, there have been no research studies to date to analyze the performance of a floor sensor system for such type of classification. From the time series acquired in pilot experiments capturing several gait cycles on the footprint imaging sensor, we engineer time-domain features and use them on a set of 14 supervised linear, non-linear, ensemble and deep machine learning models. These aim to achieve reliable classification scores for 10 different pre-defined manners of walking, enacted by a single user, to provide unique gait patterns resulting in variations in the frequency content and amplitude of the temporal signal.

The rest of the paper is organized as follows: section II provides the relevant background on floor sensor system applications, the purpose of machine learning systems in the context of this work and the description of the footprint imaging sensor system. Section III formulates the problem and presents the methods, defining the manners of walking, the time domain features and the database description. Further, the machine learning features are defined, along with evaluation metrics, for the machine learning models. The results are presented in section IV, which includes a description of the machine learning models and their optimal hyper-parameters found by exhaustive search per model and offers a deeper insight into the best model found. Finally, the conclusions and future directions of this work are presented in section V.

Manuscript received February 22, 2016; revised June 7, 2016; accepted June 8, 2016. Date of publication June 21, 2016; date of current version November 17, 2016. This work was supported in part by the U.K. Engineering and Physical Sciences Research Council through the Knowledge Transfer Scheme and in part by the Consejo Nacional de Ciencia y Tecnología under Grant 467373. An earlier version of this paper was presented at the IEEE Sensors Conference, Busan, South Korea, 2015, and was published in its Proceedings (doi: 10.1109/ICSENS.2015.7370174). The associate editor coordinating the review of this paper and approving it for publication was Dr. Ryutaro Maeda. *(Corresponding author: Omar Costilla-Reyes.)*

O. Costilla-Reyes and K. B. Ozanyan are with the School of Electrical and Electronic Engineering and Photon Science Institute, University of Manchester, Manchester M13 9PL, U.K. (e-mail: omar.costilla.reyes@gmail.com).

P. Scully is with the School of Chemical Engineering and Analytical Science and Photon Science Institute, University of Manchester, Manchester M13 9PL, U.K.

Digital Object Identifier 10.1109/JSEN.2016.2583260

II. Background

A. Gait Classification With Floor Sensor Systems

Headon and Curwen [10] recognized movements undertaken by a single user by analyzing the changes in the Ground Reaction Force (GRF), in a fixed position on a weight- sensitive floor, resulting from jumping, sitting and rising. A hidden Markov model was used for classification with performance approaching 100%. A disadvantage of this study is that the postural activities were performed statically at the same position, thus excluding gait analysis in the temporal domain.

For the purpose of classification of human postural and gestural movements using floor sensor systems, Saripalle et al. [11] employed force platforms to infer the center of pressure of individuals. 11 body movements by volunteers were classified with an accuracy ranging from 79% to 92% using linear and non-linear supervised machine learning models. Feature selection is emphasized as a critical step for obtaining reliable accuracy scores, but this approach is limited by the lack of a single classification model suitable for all types of movement.

In a study of gait analysis for biometric applications, Vera-Rodriguez et al. [12] used a piezoelectric sensor system with two sensor pads to capture a single footfall period (right and left steps) at a high sampling frequency speed (1.6 KHz). The pads comprise 88 sensors each. A biometric system was constructed to analyze the largest footstep database to date according to the authors, with nearly 20,000 footstep sequences from 127 users. The time and space domain analyses are fused at the score level, yielding an equal error rate of 7.1%, which the authors claim is the best for a biometric application using a floor sensor system. This approach limits the data to a single gait cycle, since it utilizes a single pair of sensing pads.

Another biometric system presented by Qian et al. in [13] is based on a floor sensor system of 96 Tekscan sensing mats, yielding a total dimension of 221 ft^2. The dataset consisted of gait data from 11 volunteers performing several characteristics of walking including normal walking, varying speed walking and free walking. The analysis is based on features created from center of pressure data in time and space domains. The classification analysis has been limited to the Fisher linear discriminant model, chosen for its simplicity in training and testing. The cost implications of utilizing the chosen sensor technology over large areas, as well as the implications of the frame rate being limited to 44 Hz, have not been addressed.

A sensor floor system for movement monitoring and falls detection in a smart home environment, described by Leusmann et al. [14], targets the improvement of independent living among the elderly population. The system consists of 240 piezoelectric sensors installed on a 20 m^2 floor surface. An overall success rate of 72% for step detection was achieved using the time domain data, in the absence of continuous steps analysis.

B. Footprint Imaging Sensor System Description

In this work we employ a 1 m × 2 m "intelligent carpet" prototype consisting of 116 POF sensor elements strategically placed, between the top pile layer and the deformable underlay of a commercial carpet, in 3 sets of parallel sensor elements, oriented at 0° (20 POF sensors), 60° and 120° (48 POF sensors each) [4], as shown in Figure 1. Light attenuation, resulting from the deformation due to the pressure exerted, is recorded separately from all 116 sensor elements comprising the sensor head, yielding a 3-angle Radon transform of the surface deformation ('depth of bending', see [4]). We have shown that the spatial and temporal data from the footprint imaging sensor allows the derivation of the main parameters of gait under unobtrusive and unsupervised conditions. Further details of the theory behind the sensor operation, the data acquisition and processing procedures, together with an example of sensor fusion for footstep imaging, are available elsewhere [4]. To perform sensor fusion in this work we use the raw data from the individual POF sensors to create temporal features, as detailed further.

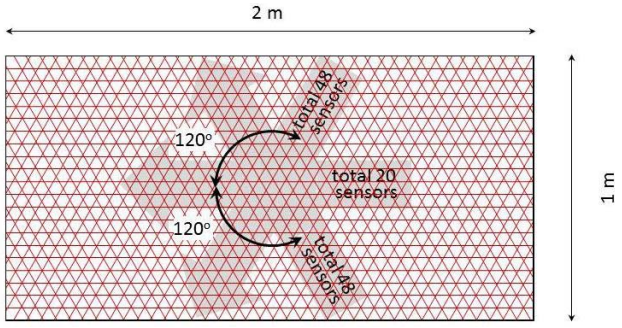

Fig. 1. Sensor head of the system. The 116 red lines across the area represent the line integrals of optical fiber attenuation, grouped in 3 angular projections to ensure consistent spatial and temporal sampling.

III. Methods

A. Data Acquisition

A LabVIEW environment was used for the sensor data acquisition from the "intelligent carpet" prototype [4]. The acquisition speed, controlled by the clock of an external Complex Programmable Logic Device (CPLD), was set to yield 256 full frames per second, each POF sensor element was polled with a period corresponding to 256 Hz. This acquisition rate is higher than the previously reported [4] and is better suited for processing of the temporal signals. The overall time window for data acquisition during each experiment was set at 5.46 seconds, or 1400 full frames at 256 Hz, allowing enough time for all manners of walking to be completely captured during the gait experiments. The latter were performed by a single healthy person walking in the direction along the length of the prototype, allowing at least 2 gait cycles (4 to 5 consecutive footsteps). A total of 855 gait experiments were captured, yielding approximately 111 million unique POF sensor signals.

B. Data Processing

The data processing and analysis (see Figure 2) was accomplished using open source software packages, including the

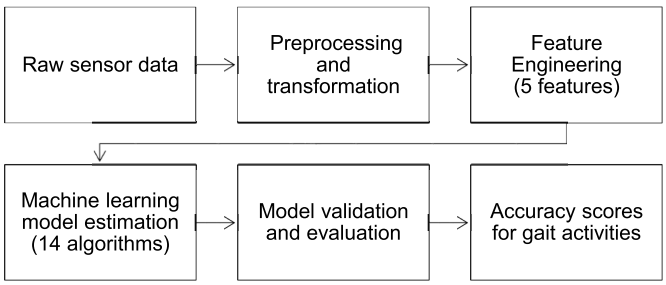

Fig. 2. The data analysis procedure. The second row shows the flow for only one model, as a representative of the 14 alternatives.

Python programming language, the NumPy/SciPy scientific computing package and the scikit-learn machine learning library [15]. The raw data was pre-processed with a Savitzky-Golay filter for smoothing. From the 855 sequences, 757 were retained after cleaning the dataset from noisy and incorrect data. The data is also scaled to a range between 0 and 1 as a required preprocessing step for some of the machine learning modes.

C. Feature Engineering

Five different types of features were engineered and tested for the time domain analysis: Spatial Average (SA), Standard Deviation (SD), Adjacent Mean (AM), Cumulative Sum (CS) and Cumulative Product (CP). The features' definition and the corresponding mathematical representations are given below.

Here t represents time, in units of frames, ranging from 0 to 1400, thus covering a time interval of 5.46 s at 256 Hz. N is the number of POF sensors and SF_i represents the signal of the i^{th} POF sensor.

1) *Spatial average:* The average of all the SF POF signals are calculated at each time step.

$$SA[t] = \frac{1}{N}\sum_{i=1}^{N} SF_i[t] \tag{1}$$

2) *Standard deviation:* The spread of the distribution of the POFs at each frame step is calculated.

$$SD[t] = \sqrt{\frac{1}{N}\sum_{i=1}^{N} (SF_i\,[t] - SA\,[t])^2} \tag{2}$$

3) *Adjacent mean:* The mean of two signals from adjacent POFs is calculated the median $SF_{N/2}$ of all the signals in each time frame and the signal with the next higher index, $SF_{N/2+1}$.

$$AM\,[t] = \frac{\mathrm{SF}_{N/2}\,[t] + \mathrm{SF}_{N/2+1}\,[t]}{2} \tag{3}$$

4) *Cumulative sum:* Cumulative summation of the POF signals at each frame step is calculated and then averaged to obtain a single value per time frame.

$$CS[t] = \frac{1}{N}\sum_{j=1}^{N}\sum_{i=1}^{j} SF_i[t] \tag{4}$$

5) *Cumulative product:* The product of the POF signals at each time step is calculated, and then the average value of the POFs is calculated to obtain a single value at each frame step.

$$CP[t] = \frac{1}{N}\sum_{j=1}^{N}\prod_{i=1}^{j} SF_i[t] \tag{5}$$

D. Temporal Gait Pattern Recognition

Two main groups of machine learning algorithms, linear and non-linear, were independently applied to the data.

1) Linear Learning Models: We considered five linear models: Support Vector Machine (SVM), Perceptron, Logistic Regression, Passive Aggressive Classifier and Stochastic Gradient Descent (SGD). The SVM model is known for its top classification performance in different application domains, including gait analysis with floor sensors systems [12], [19]. In this paper, we used two implementations of the SVM algorithm [15]; the first one (LIBLINEAR) prioritizes the loss and regularization whilst the other (LIBSVM) allows different kernel schemes and operates on a one-to-one scheme for multiclass classification.

2) Non-Linear, Ensemble and Deep Learning Models: We considered Decision Trees and Extra Trees classifiers, as well as the similarity-based K-Nearest Neighbors method [19]. Algorithms based on boosting techniques, such as AdaBoost and Gradient Boosted Regression Trees (GBRT), were also considered, together with the Random Forest algorithm which is based on training a set of de-correlated decision trees classifiers [19]. We also considered two types of deep learning models: a deep feed forward Artificial Neural Network (ANN) and a Recurrent ANN.

3) Classes and Model Performance Optimization: The 10 manners of walking, are defined in Table I. We use supervised learning to find the best approximation function $h(x)$ (hypothesis) to a desired function $f(x)$ that correctly maps input sensor data x to a manner of walking y in a supervised way. The challenge for the machine learning models is to find the approximation $h(x)$ of $f(x)$, with the highest classification accuracy, as indicated by the performance classification scores for each model with optimized hyper-parameters. The latter were optimized via exhaustive search and their classification performance was quantified for each of the engineered machine learning features (SA, SD, AM, CS and CP) by cross validation [17], expressed as mean validation score for the 10 manners of walking.

Figure 3 shows three time sequences, for normal, slow and fast gait. The SA feature is used in the figure. The data sampling rate is illustrated by using the time frame number on the horizontal axis. The start and end of the sequences, as defined by the signals observed at the maximum amplitude 2.604, coincide with the user stepping on and off the sensor head, respectively. The pattern variation resulting from the change in cadence for the three sequences is clearly observed.

Figure 4 shows a normal gait sequence (class 1, see Table I) with identified events in a single gait cycle. The shape of the signal is unique for the footprint imaging sensor system and is due to the variation of light transmission in the sensor elements as a result of the floor surface deformation. The amplitude

TABLE I

RELATIONSHIP BETWEEN CLASSES, MANNERS OF WALKING AND DATA ACQUISITION DETAILS

Class	Experiment	Manner of walking	Steps	Total samples
1	Normal Gait	Walking at normal speed and gait frequency (cadence).	4	92
2	Slow Gait	Lower constant speed and cadence compared to 1.	4	84
3	Fast Gait	Higher constant speed and cadence compared to 1.	3	105
4	Barefoot Gait	Normal gait, but with modified GRF distribution leading to a change in the shape and amplitude of the signals.	4	88
5	Gait with Weight	Normal gait attempted while carrying a 10 kg bag with both hands. This increases the amplitude modulation of the temporal signal and modifies the spatial distribution of pressure due to increased weight.	4	86
6	Gait with Hands behind Back	Normal gait attempted with hands crossed behind the back. The normal walking pattern is affected by the modified posture (shift of the center of pressure locus) and the lack of arm swings.	4	82
7	Backwards Gait	Modified walking pattern, cadence, stride and center of pressure locus	4 or 5	78
8	Right Foot Leading Gait	One step at a time, with the right leg leading. Creates asymmetry in the stance phase, as e.g. in antalgic gait, leading to a reduced right leg stance phase.	4 or 5	54
9	Left Foot Leading Gait	One step at a time, with the left leg leading. Creates asymmetry in the stance phase, as e.g. in antalgic gait, leading to a reduced left leg stance phase.	4 or 5	46
10	Side Gait	Walking sideways, with the coronal plane aligned with the direction of movement (either leg leading).	4 or 5	42

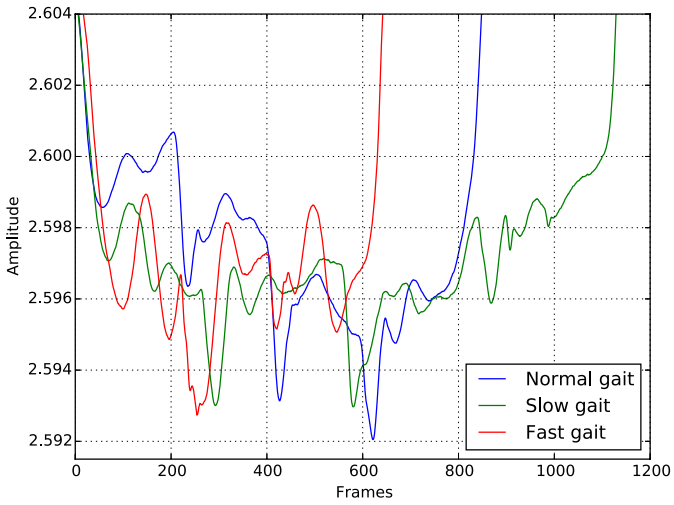

Fig. 3. Temporal sequences for normal, slow and fast gait (classes 1, 2 and 3 in Table 1).

in Figure 4 is calculated as the signal average at each time frame step. The timing of the events shown can be extracted automatically for further use in gait analysis.

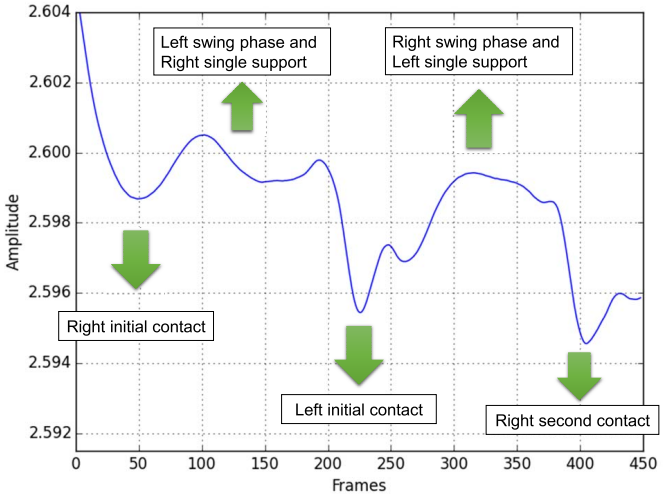

Fig. 4. Identification of gait events in the temporal signals. Right and left refer to the right and left foot respectively.

TABLE II

BEST PERFORMANCE OVERALL MODELS BY FEATURE

Feature	Algorithm	Mean validation score
Spatial Average	Extra Trees Classifier	77.01 ± 04.79 %
Cumulative Product	Extra Trees Classifier	76.98 ± 07.85 %
Cumulative Sum	SVM (LIBSVM)	85.45 ± 07.12 %
AM	Random Forest	90.84 ± 02.46 %
STD	Extra Trees Classifier	74.77 ± 05.88 %

IV. RESULTS AND DISCUSSION

Models from a simple linear Perceptron to complex Random Forests and deep ANNs are parametrized and optimized for classification performance, with regard to the temporal sensor data and calculated features.

A. Model Performance Evaluation

The 10 scores obtained per 10-fold cross-validation experiment are averaged to provide a unique mean validation score. The standard deviation of the 10 scores per model evaluation is also calculated to provide confidence intervals. For the best overall model selected, the classification performance is also expressed as the precision (exactness), recall (completeness) and F-score, (the harmonic mean of precision and recall) to provide further insight into the model's performance.

Table II displays the best performance scores for each of the 5 features used across all models. The tuned Random Forest model with an AM feature was the top performing model-feature pair with a mean validation score of 90.84 ± 2.46 %. This compares to the single decision tree models yielding a mean validation score of 82.30 ± 6.93 %.

Table III shows the classification performance of the linear learning models using the best feature found per experiment. The best mean validation score was of 85.45 ± 7.12 % for SVM (LIBSVM) with a CS feature. This model uses a linear kernel with optimized regularization and tolerance as detailed in Table III.

Table IV shows the classification performance of the non- linear and ensemble learning models, along with the best model's hyper-parameters found by grid search for

TABLE III
LINEAR LEARNING MODELS' BEST HYPER-PARAMETERS AND PERFORMANCE

Model	Feature	Hyper-parameters			Mean validation score
Perceptron	**STD**	Penalty: **L2**	Alpha: **0.0001**	Iterations: **8**	**52.44 ± 6.38 %**
Passive aggressive	**STD**	Loss: **L2**	C: **0.0001**	Iterations: **8**	**55.88 ± 5.88 %**
SGD	**STD**	Penalty: **L2**	Alpha: **0.0001**	Loss: **Squared Hinge**	**59.18 ± 4.68 %**
Logistic Regression	**Cumulative Sum**	Penalty: **L1**	C: **1**	Solver: **Newton-cg**	**69.89 ± 9.01 %**
SVM (LIBLINEAR)	**Cumulative Sum**	Multi-class: **Crammer Singer**	C: **1**	Loss: **Squared Hinge**	**79.42 ± 9.28 %**
SVM (LIBSVM)	**Cumulative Sum**	Kernel: **Linear**	C: **200**	Tolerance:**0.001**	**85.45 ± 7.12 %**

TABLE IV
NON-LINEAR AND ENSEMBLE LEARNING MODELS' BEST HYPER-PARAMETERS AND PERFORMANCE

Model	Feature	Hyper-parameters			Mean validation score
AdaBoost	**AM**	Learning Rate: **1**	N-estimators: **900**	Algorithm: **SAMME**	**67.11 ± 5.64 %**
K-Neighbors	**AM**	N-neighbors: **3**	Weights: **Distance**	Algorithm: **Ball Tree**	**75.43 ± 4.45 %**
Decision Tree	**AM**	Max-features: **Auto**	Criterion: **Gini**	Max-depth: **60**	**82.30 ± 6.93 %**
Gradient boosting	**AM**	N-estimators: **600**	Learning Rate: **0.1**	Max-depth: **3**	**86.92 ± 5.82 %**
Extra Trees	**AM**	Max-features: **Log2**	N-estimators: **500**	Criterion: **Gini**	**87.98 ± 5.33 %**
Random forest	**AM**	Max-features: **Log2**	N-estimators: **150**	Criterion: **Entropy**	**90.84 ± 2.46 %**

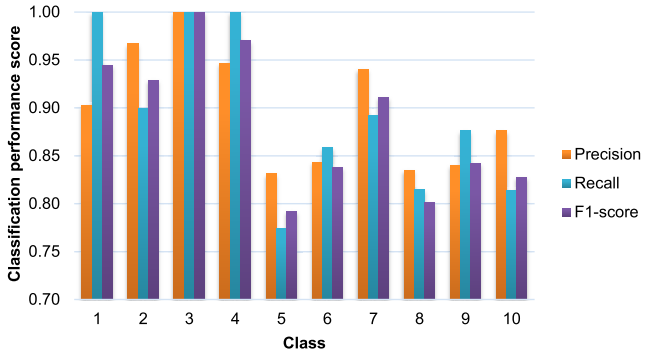

Fig. 5. Performance per class for the Random Forest model.

the best model - feature combinations. The Random Forest model with the AM feature is the overall best performer. (see also Table II). The theoretical background of the linear and non-linear models presented in Tables II and III is provided in [18] and [19].

The performance analysis of the deep feedforward ANN and the recurrent ANN are presented in section IV.C.

B. Analysis of the Classification Results

The five temporal features are introduced in section IIIC and listed in Table II. The AM feature, which manifests the best classification performance overall, utilizes the average of two adjacent POF signals. The rationale in the construction of this feature is that adjacent parallel POFs on the sensor (see Figure 1) ensures that the footprint is captured, as their separation is smaller than the width of an adult foot. The remaining time features in section IIIC use all POF signals within the time frame and differ by the particular calculations involved. Thus it may be speculated that the optimal performance of the AM feature is due to much better signal-to-noise ratio.

1) Performance by Class of the Optimal Model: The mean validation scores per class of the Random Forest model can be observed in Figure 5. The cross-validated confusion matrix of the model is shown in Figure 6. The fast gait pattern (class 3) obtained the best F-score of nearly 100% while the gait with weight pattern (class 5) performed the worst overall obtaining a F-score of 83%. For this class, the total number of incorrectly predicted samples was 20, which was the highest. From those samples, the highest number assigned to a single class was 11, the hands behind the back gait pattern (class 6). The average classification performance across all the classes yields the following mean validation scores: precision of 91.74 ± 2.45%, recall of 90.89 ± 2.44% and F-score of 90.84 ± 2.46%. Those were the best performance results across all 5 features used.

2) Optimal Model Learning Curve: Figure 7 shows the machine learning curve for the optimal Random Forest model that manifested the best overall classification performance. The red and green graphs indicate the train scores and cross-validation scores, respectively, as a function of training examples. The corresponding confidence intervals for the scores are also plotted, indicated as shadowing on the curves. A 10-fold cross-validation was used to calculate the scores, as in section IV.A. The training examples vary from 0 to 757 samples, the later corresponding to the entire dataset.

This particular model provides high training classification performance early on. This is expected for an ensemble learning model. The cross-validation score increases as a function of sample size reaching a steady value of 90% for a training set of 530 samples onwards.

C. Deep Learning Models Analysis

Recently, deep machine learning models have shown top tier performance results for classification tasks in the fields of vision, speech recognition, and handwritten digits recognition [20]. The models take advantage of the ongoing decline of price of high performance computational systems and the

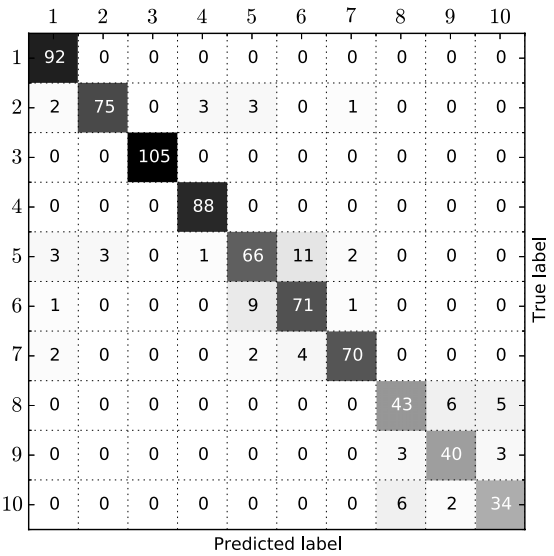

Fig. 6. Confusion matrix for the Random Forest model.

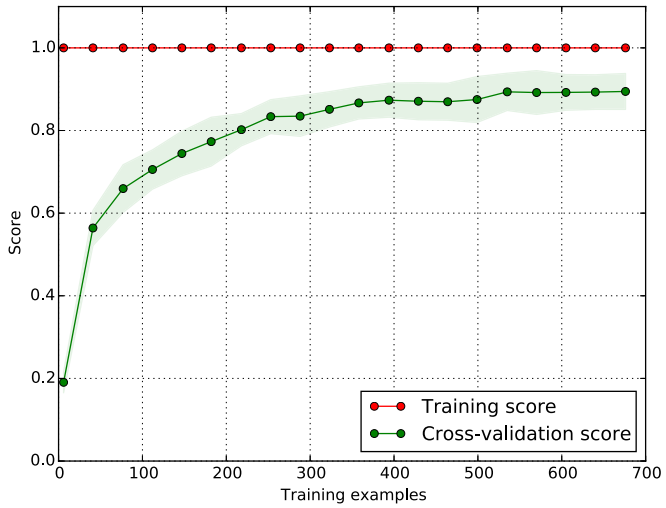

Fig. 7. Identification of gait events in the temporal signals. Right and left refer to the right and left foot respectively.

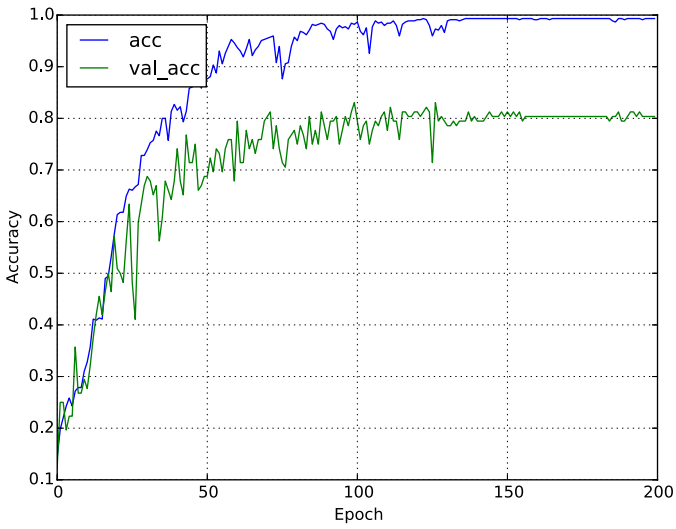

Fig. 8. Deep neural net training and validation accuracy.

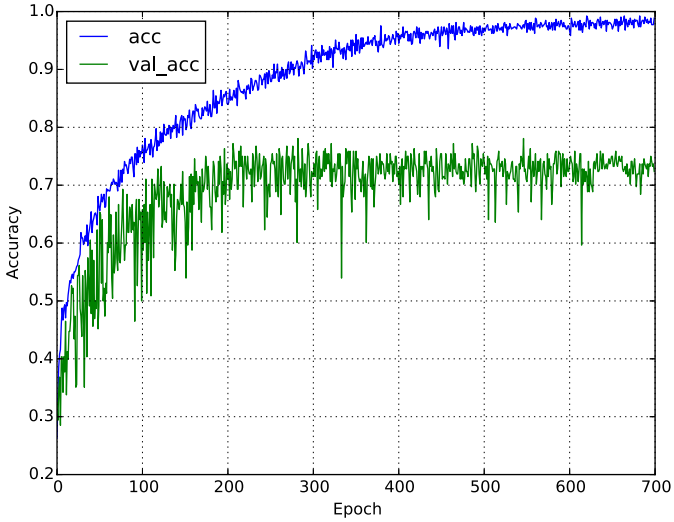

Fig. 9. Recurrent neural net training and validation accuracy.

increase availability of data to design powerful and sophisticated ANNs for pattern identification. In this paper, deep learning models are tested for effectiveness with the footprint imaging sensor data.

A deep feed-forward ANN and a recurrent ANN were designed, trained and tested with the temporal data features presented in this paper. The Python-based deep learning library Theano [21] was used for the design of the deep ANN models. The deep learning models training, testing and optimization operations were performed entirely on a NVIDIA Titan X GPU for parallel processing, thus reducing the model computation time.

1) Deep Feed Forward ANN: A 10 hidden layer ANN architecture with 256 hidden units per layer was found to be the most suitable for our type of temporal data. The initialization of the layer's weights follows the random distribution suggested by Glorot and Bengio [22]. The rectifier linear unit (ReLu) [23] is used as activation function in the ANN's hidden units at each layer except for the last, which uses a softmax [24] activation function to transform class scores to probabilities. An Adagrad optimizer function is used with default hyper-parameters [25] to optimize the ANN's nodes weights at each epoch. 200 epochs were performed using a batch size of 16 training samples. A 70-30 train-test split was adopted.

The top classification score was obtained for the CS feature. The average classification performance of all the classes yields 82% precision, 80% recall and 80% F-score. The training and validation accuracies as a function of epoch optimization are shown in Figure 8.

2) Recurrent ANN With ReLus: The temporal data from the footprint imaging sensor was used to train a recurrent ANN architecture where the weights of the network are initialized by using the identity matrix in the hidden units, as suggested by Le et al. [26]. The novelty of our approach in this experiment is the assumption that a sequence learning model is appropriate,

given the sequential nature of our features calculated from the raw sensor temporal data.

The ANN was designed with 2000 hidden units, batch size of 16 training samples and learning rate set at 10^{-6} by using an Adagrad optimizer. The network optimization ran for 700 epochs until convergence. The top classification score for this experiment was obtained for the AM feature. The average classification performance of all the classes is 75 % precision, 72 % recall and 72 % F-score. The training and validation accuracies per epoch are shown in Figure 9.

V. Conclusion and Future Directions

In this paper, a methodology was presented to test the capability of a unique footprint imaging sensor system (the "Intelligent Carpet" [4]) to provide useful time domain data of human gait. The methodology was based on the use of state-of-the-art machine learning models and feature engineering. We conclude that the time domain data from the footprint imaging sensor system allows reliable classification of human gait and that the selection of model-feature pairs is essential to obtain high classification scores.

The 10 manners of walking, repeatedly enacted by a single person to yield a dataset of 757 time sequences, were chosen for their influence on the sensor signal output: as straightforward examples, experiments at normal, slow and fast gait vary the frequency content of the signals, while experiments with barefoot gait and gait while carrying weight modify the amplitude. This choice of manners of walking can be further refined, for example by maximizing their clinical relevance.

Five types of time series features were engineered and fourteen different types of machine learning models with tuned hyper-parameters were applied to analyze these features. The hyper-parameters' tuning was performed by grid search and performance evaluation with a 10 fold cross-validation with confidence intervals. The best classification performance with a mean validation score of 90.84 ± 2.46 % was observed for the Random Forest model with tuned hyper-parameters, using an AM feature. The results imply that the choice of model and the feature design affect strongly the time-domain analysis, highlighting the importance of model-feature pairing and the role of hyper-parameter optimization.

One of the most important insights gained from the experiments in this work, prompted by the high performance of the AM feature, is that only a couple of the 116 POF sensors in the footprint imaging sensor are sufficient to obtain reliable mean validation scores for the presented type of gait activities. A future analysis of the data can determine the exact subset of POFs necessary to yield the best classification scores from temporal data. The knowledge of this subset of POFs may influence the design and the principles of data acquisition in future embodiments of the footprint imaging sensor.

The deep learning models, which included a deep feed-forward ANN and a recurrent ANN for sequence learning, outperform some, but not all, of the shallow learning models. We argue that this is due to the limited data available and the lack of consideration for the spatial component. Deep learning models manifest top tier classification performance in problems involving large amounts of data [20]; thus, improved classification may be expected from such models in future experiments with substantially larger gait datasets.

The data analysis presented in this paper is limited to pre-defined time-domain features. Future analyses may involve classification analysis of gait data in the spatial domain from reconstructed tomographic images of the footsteps delivering pressure information assigned to location. Fusion of the spatial and time domain data will also be considered.

A promising use of the footprint imaging sensor is for healthcare applications. In addition to the potential to accumulate unobtrusively vast longitudinal data on individual users under routine everyday conditions, changes in their gait can be analyzed at any time while performing cognitively demanding tasks, e.g. dual-task gait experiments [27]. The extent to which the footprint imaging sensor can detect clinically significant gait changes is of current and future research interest and will be addressed in our future experiments with a significant number of volunteers performing simple and complex tasks. This direction has the potential, for example, to detect the early onset of illness affecting the executive function of the brain and thus mobility. Further obvious applications are in rehabilitation, sports and security.

Acknowledgment

The author O. Costilla-Reyes would like to acknowledge CONACyT (Mexico) for a studentship and Dr. Paul Wright for help with programming the CPLD.

References

[1] D. Gafurov, "A survey of biometric gait recognition: Approaches, security and challenges," in *Proc. Annu. Norwegian Comput. Sci. Conf. Citeseer*, 2007, pp. 19–21.

[2] P. Rashidi and A. Mihailidis, "A survey on ambient-assisted living tools for older adults," *IEEE J. Biomed. Health Informat.*, vol. 17, no. 3, pp. 579–590, May 2013.

[3] K. B. Ozanyan, S. G. Castillo, and F. J. P. Ortiz, "Guided-path tomography sensors for nonplanar mapping," *IEEE Sensors J.*, vol. 5, no. 2, pp. 167–174, Apr. 2005.

[4] J. A. Cantoral-Ceballos, N. Nurgiyatna, P. Wright, J. Vaughan, C. Brown-Wilson, P. J. Scully, and K. B. Ozanyan, "Intelligent carpet system, based on photonic guided-path tomography, for gait and balance monitoring in home environments," *IEEE Sensors J.*, vol. 15, no. 1, pp. 279–289, Jan. 2015.

[5] G. V. Zammit, H. B. Menz, and S. E. Munteanu, "Reliability of the TekScan MatScan system for the measurement of plantar forces and pressures during barefoot level walking in healthy adults," *J. Foot Ankle Res.*, vol. 3, no. 11, 2010.

[6] B. Bilney, M. Morris, and K. Webster, "Concurrent related validity of the GAITRite walkway system for quantification of the spatial and temporal parameters of gait," *Gait Posture*, vol. 17, no. 1, pp. 68–74, Feb. 2003.

[7] T. Kleinberger, M. Becker, E. Ras, A. Holzinger, and P. Müller, "Ambient intelligence in assisted living: Enable elderly people to handle future interfaces," in *Universal Access in Human-Computer Interaction. Ambient Interaction*. Springer, 2007, pp. 103–112.

[8] M. Ziefle, S. Himmel, and W. Wilkowska, "When your living space knows what you do: Acceptance of medical home monitoring by different technologies," in *Information Quality in e-Health* (Lecture Notes in Computer Science), vol. 7058, A. Holzinger and K.-M. Simonic, Eds. Springer, pp. 607–624, 2011.

[9] C. Brown Wilson, J. C. Ceballos, P. Wright, J. Vaughan, C. Todd, P. J. Scully, and K. B. Ozanyan, "Developing a sensing solution to reduce the risk of falls for older people: An interdisciplinary approach," *Gerontechnology*, vol. 13, no. 2, p. 174, 2014.

[10] R. Headon and R. Curwen, "Recognizing movements from the ground reaction force," in *Proc. Workshop Perceptive Interfaces ACM*, 2001, pp. 1–8.
[11] S. K. Saripalle, G. C. Paiva, T. C. Cliett, III, R. R. Derakhshani, G. W. King, and C. T. Lovelace, "Classification of body movements based on posturographic data," *Human Movement Sci.*, vol. 33, pp. 238–250, Feb. 2014.
[12] R. Vera-Rodriguez, J. S. D. Mason, J. Fierrez, and J. Ortega-Garcia, "Comparative analysis and fusion of spatiotemporal information for footstep recognition," *IEEE Trans. Pattern Anal. Mach. Intell.*, vol. 35, no. 4, pp. 823–834, Apr. 2013.
[13] G. Qian, J. Zhang, and A. Kidané, "People identification using floor pressure sensing and analysis," *IEEE Sensors J.*, vol. 10, no. 9, pp. 1447–1460, Sep. 2010.
[14] P. Leusmann, C. Möllering, L. Klack, K. Kasugai, M. Ziefle, and B. Rumpe, "Your floor knows where you are: Sensing and acquisition of movement data," in *Proc. 12th IEEE Int. Conf. Mobile Data Manage. (MDM)*, vol. 2, Jun. 2011, pp. 61–66.
[15] F. Pedregosa, G. Varoquaux, A. Gramfort, V. Michel, B. Thirion, O. Grisel, and J. Vanderplas, "Scikit-learn: Machine learning in Python," *J. Mach. Learn. Res.*, vol. 12, pp. 2825–2830, Oct. 2011.
[16] O. Costilla-Reyes, P. Scully, and K. B. Ozanyan, "Temporal pattern recognition for gait analysis applications using an 'intelligent carpet' system," in *Proc. IEEE SENSORS*, Nov. 2015, pp. 1–4.
[17] R. Kohavi, "A study of cross-validation and bootstrap for accuracy estimation and model selection," *IJCAI*, vol. 14, no. 2, 1995.
[18] C. Bishop, *Pattern Recognition and Machine Learning*, vol. 16. New York, NY, USA: Springer, 2006, p. 049901.
[19] H. Trevor, R. Tibshirani, and J. Friedman, *The Elements of Statistical Learning: Data Mining, Inference and Prediction*, vol. 1.8. New York, NY, USA: Springer, 2001, pp. 371–406.
[20] Y. LeCun, Y. Bengio, and G. Hinton, "Deep learning," *Nature*, vol. 521, no. 7553, pp. 436–444, May 2015.
[21] J. Bergstra, O. Breuleux, F. Bastien, P. Lamblin, R. Pascanu, G. Desjardins, and Y. Bengio, "Theano: A CPU and GPU math compiler in Python," in *Proc. 9th Python Sci. Conf.*, Jun. 2010, pp. 1–7.
[22] X. Glorot and Y. Bengio, "Understanding the difficulty of training deep feedforward neural networks," in *Proc. Int. Conf. Artif. Intell. Statist.*, 2010, pp. 249–256.
[23] V. Nair and G. E. Hinton, "Rectified linear units improve restricted Boltzmann machines," in *Proc. 27th Int. Conf. Mach. Learn. (ICML)*, 2010, pp. 807–814.
[24] Y. A. LeCun, L. Bottou, G. B. Orr, and K.-R. Müller, "Efficient backprop," in *Neural Networks: Tricks of the Trade*. Springer, 2012, pp. 9–48.
[25] J. Duchi, E. Hazan, and Y. Singer, "Adaptive subgradient methods for online learning and stochastic optimization," *J. Mach. Learn. Res.*, vol. 12, pp. 2121–2159, Feb. 2011.
[26] Q. V. Le, N. Jaitly, and G. E. Hinton. (2015). "A simple way to initialize recurrent networks of rectified linear units." [Online]. Available: http://arxiv.org/abs/1504.00941
[27] J. M. Hausdorff, A. Schweiger, T. Herman, G. Yogev-Seligmann, and N. Giladi, "Dual-task decrements in gait: Contributing factors among healthy older adults," *J. Gerontol. A, Biol. Sci. Med. Sci.*, vol. 63, no. 12, pp. 1335–1343, 2008.

Omar Costilla-Reyes received the B.Sc. degree (Hons.) in electronics engineering from Universidad Autonoma del Estado de Mexico, Mexico, in 2011, and the M.Sc. degree in electrical engineering from the University of North Texas, TX, USA, in 2014. During his master's studies, he was a Research Assistant in projects with funding from the National Science Foundation and National Aeronautics and Space Administration. He is currently pursuing the Ph.D. degree in electrical and electronic engineering with the University of Manchester, Manchester, U.K. He has published papers in the fields of indoor positioning, bioinformatics and robotics. His research interest lies in the intersection of machine learning, sensor systems and healthcare. He received the Best Student Paper Award in optical sensing applications at the 2015 IEEE Sensors Conference. He has won scholarships and awards for academic achievement including an academic scholarship for his master's and doctorate studies from the Mexican Science Council (CONACyT).

Patricia Scully received the B.Sc. (Hons.) degree in physics from the University of Manchester, Manchester, U.K., in 1985, the M.Sc. degree in instrumentation and analytical science from the University of Manchester Institute of Science and Technology, Manchester, in 1986, and the Ph.D. degree in electrical engineering and electronics from the University of Liverpool, Liverpool, U.K., in 1992. She was a Lecturer, a Senior Lecturer, and a Reader with Liverpool John Moores University, Liverpool, from 1990 to 2002, and is currently a Senior Lecturer in sensor instrumentation with the School of Chemical Engineering and Analytical Science, University of Manchester. Her research interests include photonic sensors and optical instrumentation, femtosecond laser writing of photonic structures, chemically sensitive optical coatings for polymers, optical sensing and measurement, optical fiber sensors, polymer optical fibers, and optical fiber technology. She is a Senior Academic/an Associate Professor with the Photon Science Institute with experience in leading industrial and research council/government funded research projects at national and international levels.

Krikor B. Ozanyan received the M.Sc. degree in engineering physics (semiconductors) and the Ph.D. degree in solid-state physics from the University of Sofia, Sofia, Bulgaria, in 1980 and 1989, respectively. He has held previous academic and research positions with the University of Sofia, the Norwegian Institute of Technology, Trondheim, Norway, the University of Hull, Hull, U.K., and the University of Sheffield, Sheffield, U.K., as well as Visiting Professorships with the University of Bergen, Bergen, Norway, and Beihang University, Beijing, China. He is currently the Director of Research with the School of Electrical and Electronic Engineering, University of Manchester, Manchester, U.K. He has been involved in projects ranging from Brewster-angle mid-IR spectroscopic ellipsometry and electron confinement in quantum wells and barriers, to the demonstration of the lasing at 333 nm from strained MQW ZnCdS/ZnS structures and *in situ* real-time optical monitoring of growth of IIIV semiconductors in MBE and MOCVD reactors. His current interests are in the area of photonic sensors for indirect imaging (tomography by optical modalities), sensor fusion, signal processing for optical experiments, and spectroscopy with ultrafast laser sources. He is a Fellow of the Institute of Engineering and Technology, U.K, and the Institute of Physics, U.K. He was a Distinguished Lecturer of the IEEE Sensors Council from 2009 to 2010, and Guest Editor of the IEEE SENSORS JOURNAL Special Issues on Sensors for Industrial Process Tomography in 2005 and THz Sensing: Materials, Devices and Systems in 2012. He is currently the Editor-in-Chief of the IEEE SENSORS JOURNAL.